Molecular Weight Dependence of the Poly(L-lactide)/ Poly(D-lactide) Stereocomplex at the Air−Water Interface

Yongxin Duan,[†] Jing Liu,[†] Harumi Sato,[‡] Jianming Zhang,[‡] Hideto Tsuji,[§] Yukihiro Ozaki,*[,‡] and Shouke Yan*[,†]

State Key Laboratory of Polymer Physics & Chemistry, Institute of Chemistry, Chinese Academy of Sciences, Beijing 100080, People's Republic of China, Department of Chemistry, School of Science and Technology, and Research Center for Environment Friendly Polymers, Kwansei-Gakuin University, Gakuen, Sanda 669-1337, Japan, and Department of Ecological Engineering, Faculty of Engineering, Toyohashi University of Technology, Tempaku-cho, Toyohashi, Aichi 441-8580, Japan

Received January 16, 2006; Revised Manuscript Received May 31, 2006

The molecular weight dependence of poly(L-lactide)/poly(D-lactide) (PLLA/PDLA) stereocomplex behavior at the air−water interface was studied by surface pressure−area (π−A) isotherms and atomic force microscopy (AFM). It was found that the compression-induced sterecomplexation of a PDLA/PLLA equimolar blend with high molecular weight ($M_w = 1 \times 10^6$ and 9.8×10^5, respectively) could occur at the air−water interface. This result is in marked contrast with the stereocomplexation of PDLA/PLLA blends in the bulk from the melt or in solutions, where the homocrystallites of either PLLA or PDLA rather than stereocomplex crystallites will be formed preferentially when the molecular weights of both polymers are higher than 1×10^5. Unexpectedly, the Langmuir−Blodgett behavior of the PDLA/PLLA blend with lower molecular weight ($M_w = 4 \times 10^3$ and 3.2×10^3, respectively), which should be favored in the stereocomplex, was distinct from that of other higher molecular weight blends. AFM images clearly disclosed for the first time the morphological changes of the equimolar blends of PLLA and PDLA at the air−water interface induced by increasing the surface pressure of the monolayer. Of particular note, the bilayer mechanism for the plateau in the isotherm was directly verified by the AFM height images.

1. Introduction

Polylactides have tremendous potential in both traditional and nontraditional applications where thermoplastics are employed because of their bioabsorbable and biocompatible properties.[1−4] They can be synthesized either as pure polyenantiomers, poly-(L-lactide) (PLLA) or poly(D-lactide) (PDLA), or as copolymers, poly-(L-lactide-*co*-D-lactide)s. Since the finding that the stereocomplexation (racemic crystallites) of PLLA and PDLA increase the melting temperature by 50 °C compared with that of crystallites of the individual homopolymers (homocrystallites) was first reported by Ikada et al.,[5] extensive investigations have been performed on the formation process and the structure of the stereocomplex.[6−11] The PDLA/PLLA stereocomplex usually occurs during their crystallization in solutions as well as in the bulk from the melt. The most common conditions required for exclusive formation of stereocomplex crystallites without formation of homocrystallites include (1) equimolar blending of D-lactide and L-lactide units,[5−8] (2) low molecular weights for both the isomeric polymers (in other words, there exists an upper critical molecular weight (about 1×10^5) below which formation of such a stereocomplex can occur in the bulk from the melt or in solutions),[6] and (3) sufficiently long sequences of both isotactic D-lactide and L-lactide units.[9,10]

X-ray diffraction studies demonstrated that the stereocomplex of PDLA/PLLA crystallizes in a triclinic unit cell ($a = 0.916$ nm, $b = 0.916$ nm, $c = 0.870$ nm, $\alpha = 109.2°$, $\beta = 109.2°$, $\gamma = 109.8°$) and the chains of PLLA and PDLA in 3_1-helical conformation are packed side by side with a monomer residue ratio of 1:1 as a result of racemic crystallization known as the β-form.[12] In contrast, the individual polyenantiomers crystallize either in a pseudoorthorhombic system with two 10_3-helices (known as the α-form)[13−15] or in a "distorted 3_1-helix α-form".[15] By force field simulation of the stereocomplex unit cells and of their powder patterns, Brizzolara et al.[16] proposed that van der Waals interactions are formed between opposite oxygen atoms and hydrogen atoms and such interactions cause the stabilization of the 3_1-helix and the higher melting point of the complex. Recently, we investigated the isothermal melt crystallization process of PLLA/PDLA by real-time infrared spectroscopy and proposed that $CH_3 \cdots O{=}C$ interaction is the driving force for forming the racemic nucleation of the PLLA/PDLA stereocomplex.[17]

Research on Langmuir−Blodgett (LB) films of polymers has increased drastically in the past decade because of possible applications in nonlinear optical devices and other fields such as biosensors and microlithography. Meanwhile, the stereocomplexation of a polymer at the air−water interface had been studied in great detail for poly(methyl methacrylate) (PMMA),[18−21] which is another typical example of a macromolecular stereocomplex. Indeed, Brinkhuis et al.[18−21] have shown that the stereocomplex could form at the air−water interface by compressing a Langmuir film of a 2:1 isotactic/syndiotactic PMMA blend. This stereocomplex consists of double-helical structures with a syndiotactic strand winding around an isotactic strand. Just recently, Pézolet et al.[22−24] published a series of papers on the investigations of the PLLA/

* To whom correspondence should be addressed. E-mail: skyan@iccas.ac.cn (S.Y.); z89016@ksc.kwansei.ac.jp (Y.O.). Phone: 0086-10-82618476. Fax: 0086-10-82618476.

[†] Chinese Academy of Sciences.

[‡] Kwansei-Gakuin University.

[§] Toyohashi University of Technology.

10.1021/bm060043t CCC: $33.50
Published on Web 09/15/2006

Table 1. Molecular Characteristics of PDLA and PLLA Utilized in This Study

code[a]	M_w	M_w/M_n	code[a]	M_w	M_w/M_n
D1	5.6×10^3	1.40	L1	4.3×10^3	1.34
D2	5.6×10^4	2.38	L2	5.0×10^4	1.79
D3	1×10^5	1.85	L3	1.5×10^5	1.80
D4	1×10^6	2.13	L4	9.8×10^5	2.04

[a] D and L represent PDLA and PLLA, respectively.

PDLA stereocomplex at the air−water interface by polarization modulation infrared reflection absorption spectroscopy (PM-IRRAS) and Brewster angle microscopy. At first, they reported that the equimolar 1:1 blend of PDLA and PLLA can form a stereocomplex at the air−water interface and has a crystal structure similar to that of the 3-D crystal of the PDLA and PLLA stereocomplex.[22] Their PM-IRRAS spectra gave clear evidence for this conclusion. Subsequently, the LB behaviors of pure PLLA and the PLLA/PDLA equimolar blend were also compared by the same techniques.[23] In the latest paper,[24] however, they reinvestigated the compression-induced stereocomplexation of PDLA/PLLA at the air−water interface with a relatively low-molecular-weight pair, and the results cast doubt on their previous conclusion on the high-molecular-weight blend. Obviously, they were aware that the molecular weight should have an effect on the stereocomplexation behavior of PDLA/PLLA at the air−water interface.

In the present study, to explore the effects of the molecular weights of PDLA and PLLA on their stereocomplexation at the air−water interface, the equimolar blends with different molecular weights are studied by coupling surface pressure−area ($\pi-A$) isotherms and atomic force microscopy (AFM). It is found that the PDLA/PLLA blend with low molecular weight ($M_w = 4 \times 10^3$ and 3.2×10^3, respectively) shows distinct LB behavior in contrast with that of other higher molecular weight blends. This means that the molecular weight dependence of PDLA/PLLA on their stereocomplexation at the air−water interface is much different from that in the bulk from the melt or in solutions. To confirm the stereocomplexation of the PDLA/PLLA blend with high molecular weight at the air−water interface, complementary structural analysis is carried out by means of the reflection−absorption infrared spectroscopy (RAIR) technique.

2. Experimental Section

2.1. Materials. The synthesis and purification of PLA used in the present study were performed according to procedures reported previously.[6−8,10] Weight-average molecular weights (M_w) and number-average molecular weights (M_n) of PDLA and PLLA are shown in Table 1.

2.2. Langmuir Film Balance Measurement. Surface pressure−area isotherms were obtained using a KSV minitrough II film balance (KSV Instrument, Helsinki, Finland) equipped with dual barriers and a Wilhelmy plate sensing device. The area of the Teflon trough is 364 × 75 mm. The subphase was doubly distilled deionized water. Thermostated water was circulated in the aluminum support of the trough to control the temperature of the subphase. The experiments were performed at 25 °C. The blend solution was prepared by the following procedure. Solutions of PLLA and PDLA with similar molecular weights were first separately prepared using chloroform (HPLC grade) to give a final concentration of 0.25 mg/mL and then admixed under stirring. The mixing ratio of the solutions was fixed at a 1:1 volume ratio. After rigorous cleaning of the water surface, polymer films were formed by spreading 35 μL of the polymer solution dropwise over the surface. Compression was initiated after a delay of 15 min to allow evaporation of the spreading solvent. The compression rate was about 0.17 (nm^2/repeat unit)/min.

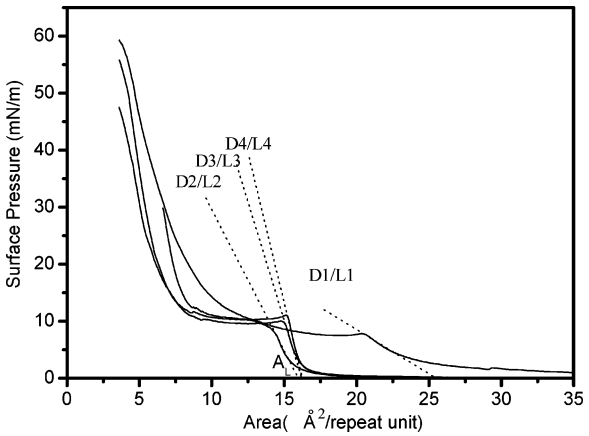

Figure 1. $\pi-A$ isotherms of PDLA/PLLA equimolar blends with different molecular weights spread at the air−water interface at 25 °C.

Transfer experiments were carried out as below. For the AFM study the substrate was newly cleaved mica, while for IR measurements, gold-sputtered glass slides were used. The substrate was first immersed into the aqueous subphase (substrate surface perpendicular to the moving barriers); after spreading of the polymer monolayer, the film was compressed until the desired surface pressure, stabilized for about 15 min, and then deposited at a constant surface pressure on the substrate. The speed of the transfer was 2 mm/min.

2.3. AFM Study. AFM measurements were carried out using a Nanoscope III MultiMode atomic force microscope (Digital Instruments) in the tapping mode. Both height and phase images were recorded simultaneously. A typical value for the set-point amplitude ratio (r_{sp}), defined as the ratio of the cantilever's oscillating amplitude to its freely oscillating amplitude was 0.7−0.9. The amplitude of the freely oscillating cantilever was approximately 40 nm. TESP tips with a resonance frequency of approximately 300 kHz and a spring constant of about 30 N/m were used. The images shown here were subjected to first-order flattening procedures to compensate for the sample tilt.

2.4. IR Measurement. The infrared measurements were carried out at a resolution of 4 cm^{-1} with a Nicholet Magna 870 spectrometer equipped with an MCT detector. To ensure a high signal-to-noise ratio, 512 scans were coadded. The RAIR spectra were obtained at an angle of incidence equal to 84°. The polarization of the incoming beam was parallel to the plane of incidence (p-polarized). All RAIR spectra were obtained by subtracting the spectrum of a Au substrate without sample from the spectrum of an LB-film-covered Au substrate.

3. Results

3.1. Isotherm Measurement. $\pi-A$ isotherms of the equimolar blends of PDLA/PLLA with different molecular weights are shown in Figure 1. The values on the abscissa in this case indicate the area per repeat unit of PLA. Obviously, the LB behavior of the D1/L1 blend, which has the lowest molecular weight among the four D/L blends, is different from that of the other three higher molecular weight blends. Some major differences between them are described as follows. First, in the low-pressure part of the isotherm, a pressure of about 0.8 mN/m can be measured even before the compression starts (at an area of 0.35 nm^2/repeat unit) for the D1/L1 blend. In contrast, for the other three blends, at an area >0.18 nm^2/repeat unit, the surface pressure is about zero and no increase in the surface pressure is observed with increasing compression. Usually, such two kinds of behavior are named as expanded and condensed monolayers, respectively. Second, extrapolations of the steeply

increasing parts before the plateau in the isotherm to $\pi = 0$ give different values of the limiting area (A_L) of the PDLA/PLLA monolayer as shown in Figure 1. The D2/L2, D3/L3, and D4/L4 blends show almost the same A_L at about 0.165 nm^2/repeat unit, which is much smaller than that of the D1/L1 blend at 0.26 nm^2/repeat unit. This difference suggests the existence of two kinds of different molecular arrangements for the PDLA/PLLA monolayer at the air−water interface depending on their molecular weights. Third, the D1/L1 blend has a relatively small surface pressure at about 7.5 mN/m for the plateau area, whereas the three higher molecular weight blends have similar surface pressures at 10 mN/m, and there is also a significant flatness of the plateau in comparison with the inclination of the plateau observed in the case of D1/L1. Moreover, the starting area for appearance of the plateau of D1/L1 is much larger than that of the other three blends.

The main difference among the isotherms of the three higher molecular weight blends is the inflection point observed prior to the plateau, which has been interpreted as a kinetic effect related to a change, typically a phase change, for which the conversion rate exceeds the compression rate.[25,26] For D4/L4, there is a sharp knee and a "dip" (a drop in the surface pressure as compression proceeds just after the onset of the transition), for D3/L3, there is a wide knee and the dip is not so obvious, and for D2/L2, the transition from the rapid increase region to the plateau region is very smooth. This difference indicates that the molecular weight affects the phase transition rate of PDLA/PLLA blends at the air−water interface.

As mentioned in the Introduction, it is well established that PDLA/PLLA stereocomplexation usually occurs during their crystallization in solutions as well as in the bulk from the melt.[5−10] There exists an upper critical molecular weight (about 1×10^5) below which formation of such a stereocomplex can take place in the bulk from the melt or in solutions.[6] That is, homocrystallites rather than stereocomplex crystallites are preferentially formed when the molecular weight of both polymers is higher than 1×10^5. From our observations, the blend with the highest molecular weight, i.e., D4/L4, behaves similar to the D3/L3 and D2/L2 systems, which are expected to form a stereocomplex. This may imply that the blend with the molecular weight of both polymers higher than the critical molecular weight as proposed by Tsuji et al. may also exhibit the ability to form a stereocomplex. Also, another interesting question may arise about why the PDLA/PLLA blend with lower molecular weights ($M_w = 4 \times 10^3$ and 3.2×10^3, respectively), which should be in favor of the formation of a stereocomplex, shows LB behavior different from that of the higher molecular weight blends. Moreover, it is noted that, for all four blends, the $\pi-A$ isotherms show an obvious plateau region. Such plateaus are often associated with phase transitions and are indicators of phase coexistence.[22] Specific to PDLA/PLLA, possibilities include a crystallization process, multilayer formation, or a conformation transition. To clarify the origin of the plateau and to find the reason for the aforementioned unexpected phenomenon, AFM measurements of the LB films were performed.

3.2. AFM Observations. Sampling of the LB films was done at different pressures, just after the solvent evaporation and before, during, and after the plateau region. The AFM results obtained on these samples indicate that no damage was caused by the AFM tip on the surface as several successive scans on the same region gave reproducible images. Because the morphological changes induced by surface pressure changes for D4/L4, D3/L3, and D2/L2 blends are similar, we only show the morphological changes of the highest (D4/L4) and lowest (D1/L1) molecular weight blends in Figures 2 and 3, respectively.

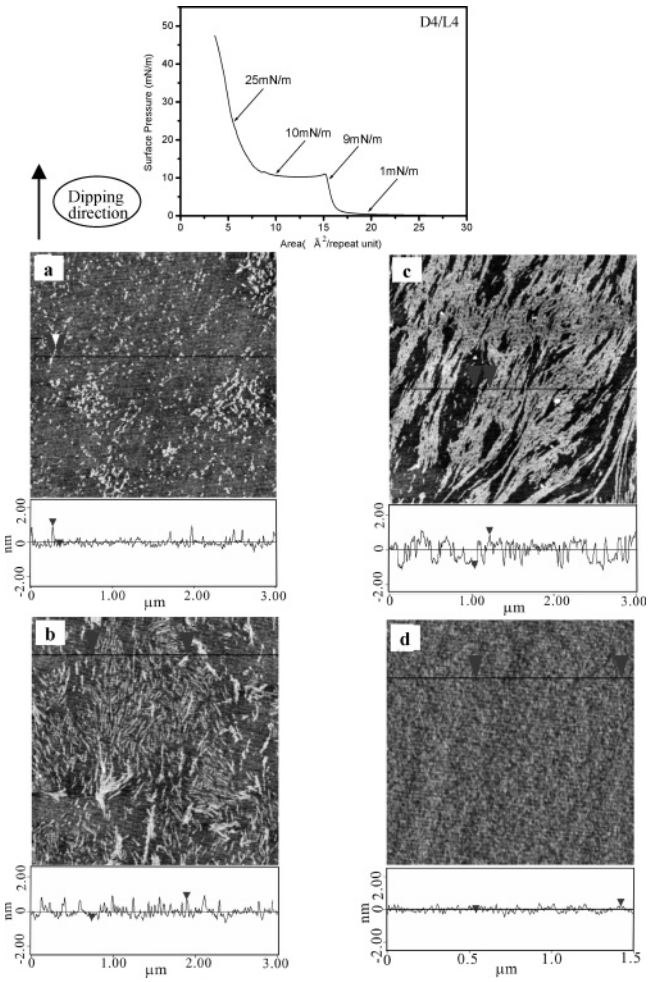

Figure 2. AFM height images of the D4/L4 blend transferred at different surface pressures shown by the arrows in the top $\pi-A$ isotherm (scale scan size 3×3 μm): (a) 1 mN/m, beginning of the first rapid increase region, (b) 9 mN/m, beginning of the plateau, (c) 10 mN/m, end of the plateau, (d) 25 mN/m, during the rapid increase region postplateau.

For the high-molecular-weight blend D4/L4, just after solvent evaporation at 0 mN/m, except for some sparsely dispersed small spots, the morphology of the sampled monolayer exhibits a smooth aspect (figure not shown). These small spots, which can always be observed for the samples collected at times before, during, and after the plateau, are most likely due to chain aggregation caused by the rapid evaporation of chloroform during spreading.

At the beginning of the first rapid increase region, see Figure 2a, one can recognize many small dots 30 nm in diameter. These small dots can aggregate to form microdomains or connect together to form dotted lines with a width of ca. 30 nm and a length from tens to hundreds of nanometers. These objects, which cover about 10% of the total surface, are surrounded by a continuous phase (corresponding to the background of the image) showing a feature similar to that of the surface sampled just after the solvent evaporation. The corresponding height profile shows that the dispersed phases are about 1.2−1.3 nm higher than the continuous phase. When the film is dipped at 9 mN/m before the plateau, see Figure 2b, a lamellar structure is the predominant morphology of the film. The height and width of the lamellae are the same as those of the dotted line shown

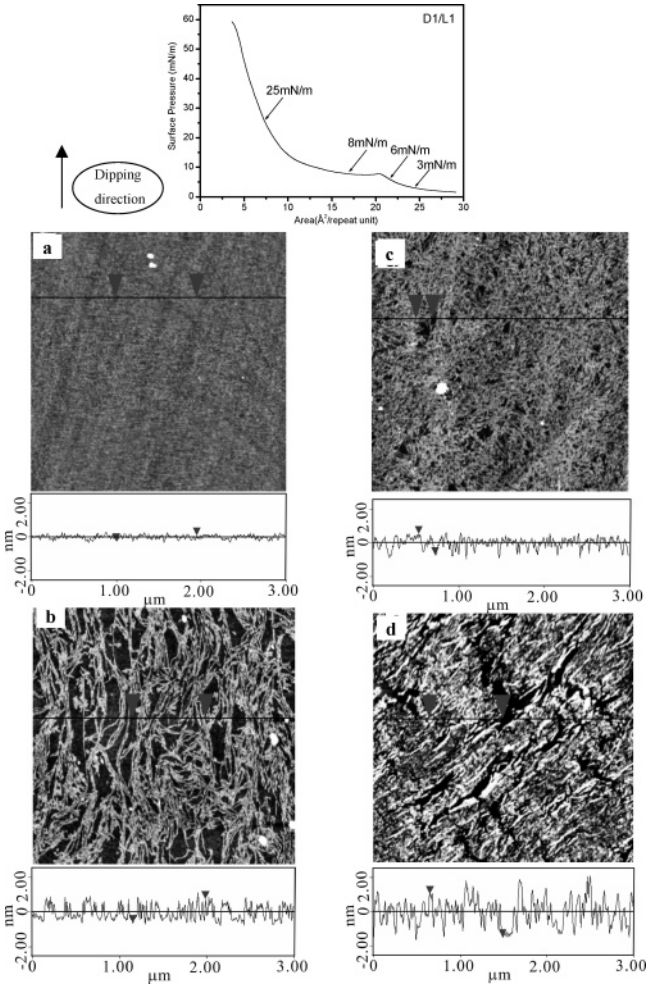

Figure 3. AFM height images of the D1/L1 blend transferred at different surface pressures shown by the arrows in the top $\pi-A$ isotherm (scale scan size 3 × 3 μm): (a) 3 mN/m, beginning of the first rapid increase region, (b) 6 mN/m, beginning of the plateau, (c) 8 mN/m, end of the plateau, (d) 25 mN/m, during the rapid increase region postplateau.

in Figure 2a. The surrounding phase still exhibits a morphology similar to that formed at low surface pressure, but a larger fraction (about 40% of the total surface) of the surface is occupied by a dispersed phase. One distinct feature in Figure 2b is the orientation of the lamellae. We found most of the lamellae are oriented along the dipping direction. For the further compressed state at the end of the plateau (Figure 2c), these lamellae become longer and connect to form a bandlike structure that has the same height as the little rods observed in the image of the phase formed at low pressure. The preferred orientation along the dipping direction can be more clearly observed. At this surface pressure, about 50% of the total surface is occupied by bandlike structures, and it is difficult to identify which one is the continuous phase. The higher phase is composed of bandlike structures, and the lower phase leads to a dual continuous phase. Figure 2d shows an image of the sample dipped at 25 mN/m (during the rapid increase region postplateau). There is only one phase, which is much finer and condensed. The corresponding height profile shows that the LB film at this pressure is much more smooth, and the AFM measurements of the film scratched by the tip on a silica wafer indicate it is a multilayer LB film with a thickness of about 4−5 nm.

AFM height images of D1/L1 dipped at different pressures are shown in Figure 3. For the monolayer transferred at 3 mN/m

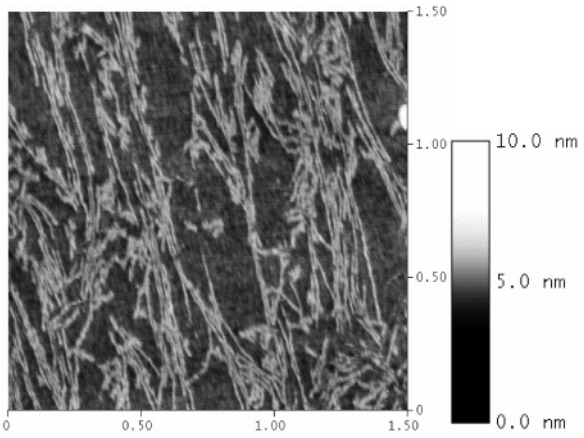

Figure 4. Enlarged AFM height images of the D1/L1 blend transferred at 6 mN/m in Figure 3b.

(Figure 3a), before the plateau, no characteristic structure is observed. Roughness analysis (*Ra* is about 0.09 nm) by AFM software and the corresponding height profile also indicate that the film transferred at this pressure is very smooth. It is very different from the case of D4/L4, which formed two phases even at low surface pressure, 1 mN/m (Figure 2a). At 6 mN/m, a two-phase structure becomes obvious in the LB film of D1/L1 (Figure 3b). The higher one is composed of many lamellae with a height of 1.2−1.3 nm, which is the same as that of D4/L4. One obvious characteristic is that the lamellae of D1/L1 are much longer than those of D4/L4 formed at the same region (Figure 2b). Some lamellae have a length of more than 1 μm, which can be observed more clearly in the enlarged image shown in Figure 4. It can be clearly seen that many lamellae united together lead to a network structure, and the orientation along the dipping direction can be observed, especially the straight part of the lamellae, which is not connected with the others. As compression proceeds, more and more lamellae are connected together. In the film dipped at 8 mN/m, network structures compose the higher phase and almost no single lamella can be observed. The percentage of the surface occupied by the higher phase increases from 40% at 6 mN/m to 80% at 8 mN/m, while the height difference between the two phases remains unchanged. An LB film transferred at 25 mN/m during the rapid increase region postplateau is more condensed, as shown in Figure 3d. Section analysis of the height image indicates that the height difference between the higher and lower phases is about 2.6 nm. Some areas with a height of about 3 nm are also found at this surface pressure.

3.3. IR Measurements. To verify that increasing the surface pressure at the air−water interface can also induce the stereocomplexation of the PDLA/PLLA blend even with high molecular weight, p-polarized RAIR (p-RAIR) spectra were measured for the D4/L4 LB multilayers dipped at the initial pressure (0 mN/m) and high pressure (25 mN/m) according to the $\pi-A$ curve shown in Figure 1. Figure 5 shows the spectra. In the low-wavenumber region, which reflects the C−C backbone vibration of PLA, a distinct band at 910 cm^{-1} characteristic of the 3_1-helical chain[28] of the PDLA/PLLA stereocomplex can be clearly observed in the spectrum of the D4/L4 LB multilayers dipped at high pressure. Sawai et al.[31] found that this band exhibits perpendicular dichroism in oriented films of β-PLLA, whereas a characteristic band of the 10_3-helical chain[28] (α-crystals) appears at a slightly higher frequency of 921 cm^{-1} and shows similarities to the 3_1-helical band at 910 cm^{-1} in shape, intensity, and dichroism. p-RAIR selects only the polarization of the incident electric field perpendicular to

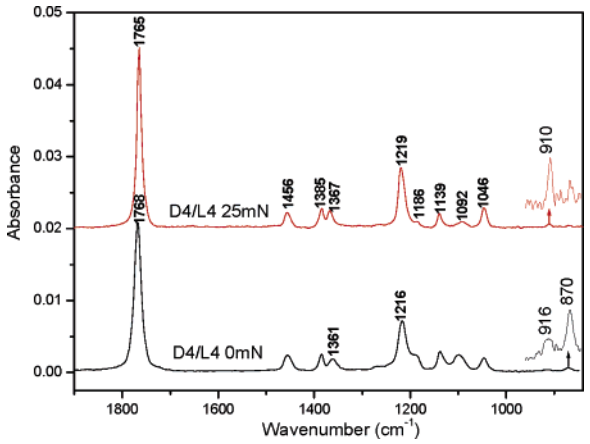

Figure 5. Reflection−absorption IR spectra of LB multilayers of the D4/L4 equimolar blend, transferred at 0 and 25 mN/m at 25 °C.

the surface of a Au substrate. Therefore, according to the "surface-selective rule" of p-RAIR spectroscopy,[29,30] only vibration modes having transition moments perpendicular to the surface appear strong in intensity, whereas modes having transition moments parallel to the surface disappear. The appearance of the band at 910 cm^{-1} rather than at 921 cm^{-1} indicates that the stereocomplexation of PDLA/PLLA with high molecular weight at the air−water interface does occur, and these 3_1-helices lie flat on the Au substrate. In contrast, in the spectrum of the D4/L4 LB multilayers dipped at the initial pressure (0 mN/m), a conformation-sensitive band at 870 cm^{-1} is more clearly identified. Usually, this band is relatively strong in the amorphous state or σ-crystals of PLA as displayed later. The very small and broad band at 915 cm^{-1} may come from the coexistence of small amounts of 3_1- and 10_1-helical chains. Due to the lack of the obvious characteristic band at 921 cm^{-1} of α-crystals, it is concluded that most of the PLLA and PDLA chains take the amorphous state at the initial pressure. In short, the spectral features in the C−C backbone vibration as shown in the inset graph of Figure 5 strongly evidence that the stereocomplex of the PDLA/PLLA blend with high molecular weight can be induced from the amorphous state with increasing surface pressure at the air−water interface.

However, it should be recognized that the well-assigned characteristic bands of the PDLA/PLLA stereocomplex in the C−C backbone vibration region are very weak and it is necessary to find other evidence for the above conclusion. In Figure 5, the C═O stretching bands at 1765 and 1768 cm^{-1} show the strongest intensity, and they are known to be sensitive to the conformation of PLA. Pézolet et al.[22] found that the 1749 and 1765 cm^{-1} bands are associated with the A and E modes of the PLA 3_1-helices in the sterecomplex, respectively. Therefore, the strong C═O stretching band at 1765 cm^{-1} and the disappearance of the band at 1749 cm^{-1} support the conclusion derived from the weak 3_1-helical band at 910 cm^{-1}. That is, the PLA 3_1-helices in the stereocomplex lie flat on the Au substrate. It seems that the band at 1765 cm^{-1} in Figure 5 provides more evidence for the pressure-induced stereocomplexation of the PDLA/PLLA blend with high molecular weight at the air−water interface. Interestingly, it is found that the peak position of the C═O stretching band in the RAIR spectrum is not a suitable characteristic band for judging the stereocomplex of PLLA and PDLA. As shown in Figure 6, in the RAIR spectra of L/D LB multilayers dipped at high pressure (25 mN/m), there is a linear shifting of the peak positions of the C═O stretching band from 1760 to 1765 cm^{-1} in different M_w pairs of the PLLA and PDLA blend. On the basis of previous spectral analysis in

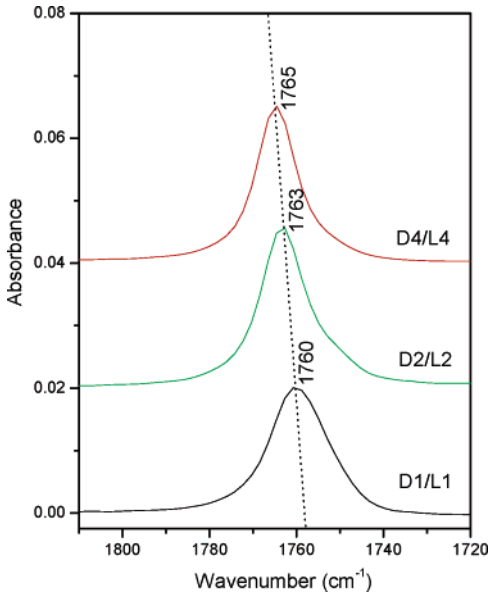

Figure 6. RAIR spectra of L1/D1, L2/D2, and L4/D4 LB multilayers dipped at high pressure (25 mN/m) in the C═O stretching vibration region.

the C−C vibration region, and the work of Pézolet et al.,[22−24] the stereocomplexes L1/D1, L2/D2, and L4/D4 at high pressure should be induced. It is surprising to find that a different peak position of the C═O stretching band in RAIR is demonstrated for the stereocomplex formed from the L/D pair with different M_w values at the air−water interface. In principle, the spectral profile of the RAIR spectrum is affected not only by the internal conformation structure but also by the spatial orientation. At present, it is not clear what the main reason is for the M_w dependence of the peak position of the C═O stretching band in the RAIR spectra of L/D LB multilayers. Nevertheless, the data in Figure 6 clearly suggest that we should take caution in using this band in RAIR spectra as a criterion for the stereocomplex of PLLA and PDLA.

Pézolet et al.[22−24] have investigated the PDLA/PLLA stereocomplex at the air−water interface by the PM-IRRAS technique. To explain their PM-IRRAS data,[22] they showed an ATR spectrum of the bulk PLLA and PDLA equimolar blend film. It is noticed that the M_w values of their PLLA and PDLA samples are 1.0×10^5 and 1.2×10^5, respectively. They thought it was the spectrum of the stereocomplex.[22] However, in fact, it was the spectrum of the homocrystalline bulk PLLA/PDLA blend rather than the PLLA/PDLA stereocomplex when such a high-molecular-weight pair was used for preparing a solution-cast film.[6] Thus, it is necessary to reinvestigate the spectral feature of the PDLA/PLLA bulk sterecomplex. For comparison, the transmission IR spectra of bulk amorphous, semicrystalline PLLA (α-form) and the PLLA/PDLA stereocomplex are listed in Figure 7. Obviously, different characteristic bands corresponding to different physical states can be easily identified in the C═O, C−O−C, and C−C stretching vibration regions as denoted in Figure 7. Among these, the bands at 1749 and 908 cm^{-1} are most distinct for the PLLA/PDLA stereocomplex as reported.[28] For making sure that the PDLA/PLLA blend with high molecular weight at the air−water interface does form the compression-induced stereocomplex, transmission IR spectra of the LB multilayers at 0 and 25 mN/m were further measured. Figure 8 depicts them. For comparison, the transmission IR (TIR) spectra of the D1/L1 LB multilayers at 0 and 25 mN/m are also included. Two conclusions can be derived from these data. First, at high pressure (25 mN/m), the existence of a band

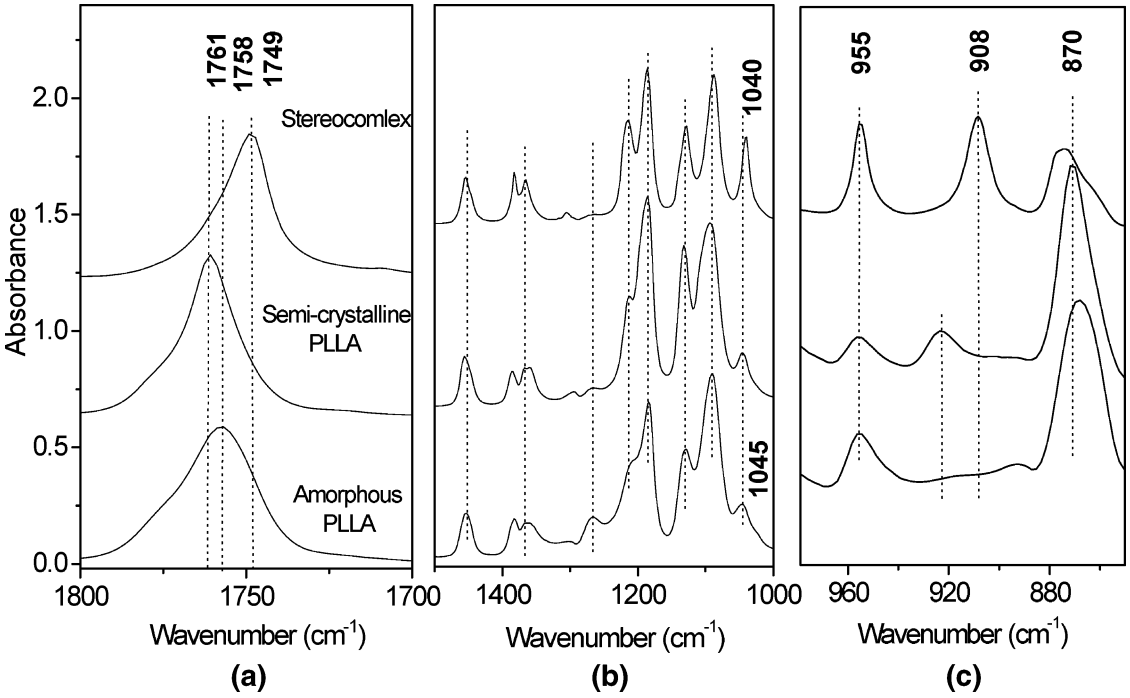

Figure 7. Comparison of the transmission IR spectra of amorphous, semicrystalline and stereocomplex PLA samples.

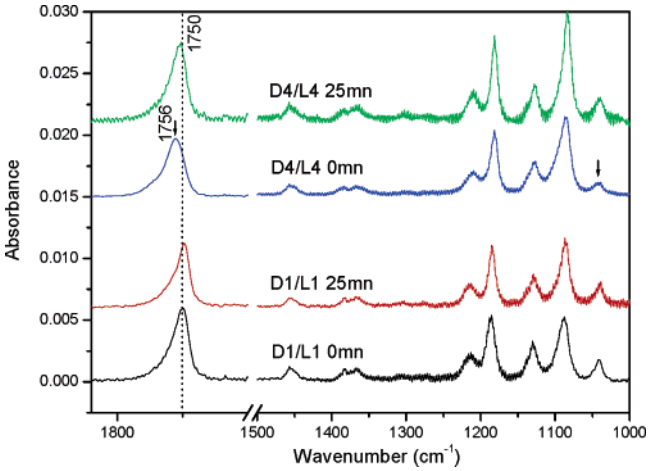

Figure 8. Comparison of the transmission IR spectra of LB multilayers of D1/L1 and D4/L4 equimolar blends, transferred at 0 and 25 mN/m at 25 °C.

at 1750 cm^{-1} for both L1/D1 and L4/D4, which is very close to 1749 cm^{-1}, indicates that both low-M_w and high-M_w pairs can ultimately form the stereocomplex at the air−water interface. Second, at the initial pressure (0 mN/m), the 1750 cm^{-1} band for L1/D1 and the 1756 cm^{-1} band for L4/D4 suggest that the initial chain conformations of PLLA and PDLA at the air−water interface before pressurizing are very different. It seems that the stereocomplex of L1/D1 already appears at the initial stage, whereas in the L4/D4 pair the PLA chains take the amorphous state, which is also evidenced by previous RAIR data.

4. Discussion

Although in several publications it is argued that the molecular weight is not very important in determining the pressure−area isotherms of polymeric materials,[32,33] varying the molecular weight of the PDLA/PLLA equimolar blends at the air−water interface yields interesting results. It is noted that the D2/L2, D3/L3, and D4/L4 blends exhibit isotherm curves similar to that reported by Bourque et al.[22] The molecular weights of the PDLA and PLLA samples they used are 1.2×10^5 and 1.0×10^5, respectively, which are between those of D3/L3 and D4/D4. By the PM-IRRAS technique, the stereocomplexation process of an equimolar mixture of PDLA/PLLA spread at the air−water interface has been in situ monitored. The RAIR and TIR spectra show that even the high-molecular-weight pair reached at 1.0×10^6 can form a compression-induced PDLA/PLLA stereocomplex at the air−water interface. This result is also supported by the same limiting area A_L at about 0.165 nm^2/repeat unit of D4/L4 as those of the D3/L3 and D2/L2 blends (see Figure 1). Bourque et al.[22] reported that, following the close-packed arrangement of the 3_1-helix chains of PDLA and PLLA in the model proposed by Brizzolara et al.,[16] the calculated area is about 0.18 nm^2/repeat unit. This value is in good agreement with our result and identifies that these isotherm behaviors of D4/L4, D3/L3, and D2/L2 should reflect an actual sterocomplexation process of PDLA/PLLA at the air−water surface.

Usually, for the bulk blend film of PDLA/PLLA prepared from the melt or a solution, homocrystallites are preferentially formed when the molecular weight of both polymers is higher than 1×10^5. However, at the air−water interface, it is found that stereocomplexation of PDLA/PLLA with high molecular weight ($M_w > 10^5$) still can be induced by increasing the surface pressure. Recently, Kikkawa et al.[34] investigated the effect of water on the surface molecular mobility of PLA thin films. Their friction force measurements and AFM observations suggested that molecular motion of both noncrystallizable and crystallizable PLA thin films on a water surface is enhanced. One piece of direct evidence was that the crystallization of PLA molecules in water took place at a lower temperature than in vacuo. This means that the physical properties such as T_g of PDLA or PLLA associated with molecular mobility will be changed at the air−water interface. The T_g of bulk PDLA or PLLA is about 69 °C, and there is a high possibility that the T_g of PDLA or PLLA reaches or becomes less than room temperature at the air−water interface, which largely increases its segment mobility. Thus,

the increasing segment mobility may be a possible reason for why high-molecular-weight equimolar blends of PDLA/PLLA form stereocomplexes more easily at the air−water interface than from the melt or a solution. However, the improved segmental mobility alone cannot explain the formation of complex crystals because when a blend of high-M_w PLLA/PDLA is crystallized from the melt, homocrystallites rather than complex crystals form although the segmental mobility is very high. Another probable reason is that the chains in this study were expanded at the water−air interface. During the compression process, such an expanded state of chains in 2-D space (the air−water interface) increases the probability of parallel arrangements between PLLA and PDLA chain segments, which induces the formation of stereocomplex crystallites even when they have a high molecular weight exceeding 1×10^6. This assumption is supported by the reported results for PLLA/PDLA fibers, where the fraction of stereocomplex crystallites increased upon heat-drawing or chain expansion.[35]

Another interesting observation in Figure 1 is the distinct isotherm of the D1/L1 blend. Compared to the other three higher molecular weight D/L blends, the D1/L1 blend displays expanded monolayer behavior rather than condensed monolayer behavior. It should be noted that the linear extrapolation of the low-pressure part of the D1/L1 isotherm is quite arbitrary, since there is no actually linear part in the isotherm at these pressures. Brinkhuis et al.[25] believed that the area obtained from the linear extrapolation of this part of the curve has no direct physical significance. The expanded monolayer behavior was described for several polymers such as isotactic poly(methyl methacrylate) (i-PMMA),[25] poly(vinyl acetate) (PVAc),[36] and poly(β-hydroxybutyrate) (PHB).[29] Lateral cohesive forces between segments of the polymer chain were argued to play an important role in this behavior.[25,29] However, the difference between the conformations of the helical chains of the PLLA and the D/L blend at the air−water interface was the main reason for their respectively expanded and condensed behaviors.[23] In fact, the 10_3-helical conformation of the PLLA homocrystals and 3_1-helical conformation of the PDLA/PLLA stereocomplex are very similar in configuration or size. In contrast, it is well-known that there is "peculiarly strong interaction" among the 3_1-helical chains of the PDLA/PLLA stereocomplex.[37] Recently, the nature of the peculiarly strong interaction between the PLLA and PDLA chains was investigated by real time infrared spectroscopy during the isothermal melt crystallization process of the PLLA/PDLA stereocomplex. A very small low-frequency shift (about 1 cm^{-1}) of $\nu_{as}(CH_3)$ and a larger low-frequency shift (about 5 cm^{-1}) of ν(C═O) were observed, and we assigned this interaction to $CH_3\cdots O{=}C$ hydrogen bonding.[17] Therefore, it seems more reasonable to propose that the different lateral interactions between the adjacent helical chains rather than the differences in helix conformation should be responsible for the respective expanded and condensed monolayer behaviors of PLLA and the D/L blend at the air−water interface. As for the D1/L1 blend, its expanded monolayer behavior at the low-surface-pressure region should be caused by the spontaneous stereocomplex between low-M_w PLLA and PDLA at the air−water interface as evidenced by Figure 8. By studying monolayers of i-PMMA, Brinkhuis et al.[25] observed that, for materials with low molecular weights, the helix formation becomes less favorable at the air−water interface. They explain this phenomenon with critical chain length effects. That is, the helix formation requires a critical chain length. Such an explanation is not suitable for the case of a low-molecular-weight D1/L1 blend at the air−water interface. According to the finding by Tsuji et al., a low-molecular-weight PDLA/PLLA blend forms stereocomplex crystallites while a higher molecular weight blend mainly forms homocrystallites from solution or the melt; it is easy to understand the spontaneous stereocomplex between low-M_w PLLA and PDLA at the air−water interface. It is also consistent with Pelletier and Pézolet et al.'s result;[24] they found that the low-molecular-weight PDLA/PLLA blends at the air−water interface should favor the stereocomplexation process and concluded that the isotherm acquired by using a low-molecular-weight PDLA/PLLA blend (1.32×10^4 and 1.45×10^4, intermediate between those of D1/L1 and D2/L2), which is similar to the isotherm of D1/L1 in Figure 1, reflects the stereocomplex process.

In Figures 2 and 3, of particular note is that all of the films sampled from the first rapid increase region to the end of the plateau have the same height between the two observed phases (1.3 nm). Interestingly, the 3_1-helix of the PLA molecule has a diameter of 1.25 nm.[22] The coincidence of the height and the diameter suggests that the objects observed are the second layer composed of the PLA molecules lying on the first layer. Therefore, the bilayer mechanism for the plateau in the isotherm proposed by Pézolet et al.[22] was directly verified by our AFM observation. It should be mentioned here that we had tried to get the electron diffraction patterns of the D/L films transferred at the beginning and the end of the plateau. Unfortunately, they disappeared very fast and were unable to be captured completely. However, we did observe a diffraction identical with that of the PDLA/PLLA stereocomplex as reported.[8] This indicates that the second layer is composed of the ordered packing of PDLA and PLLA in the crystal unit. Thus, the plateau can also be attributed to a 2-D crystallization process of the stereocomplex. The AFM images (Figures 2d and 3d) clearly display that further compression leads to the 3-D crystallization.

It should be pointed out that, for the samples dipped before the rapid increase region, the films have an orientation along the dipping direction, as shown in Figures 2 and 3. A 90° rotation of the substrate with respect to the barrier (substrate surface perpendicular to the moving barrier instead of parallel to it) produces the same results, indicating that the lateral orientation observed is not caused by a preferential orientation in the monolayer on the water surface due to the direction of the movement of the moving barrier.

5. Conclusion

By use of $\pi-A$ isotherms and AFM, it was found that the effect of the molecular weights on PDLA/PLLA stereocomplexation at the air−water interface is very different from that of the bulk PDLA/PLLA blends in the melt or solutions. First, compression-induced sterecomplexation of a PDLA/PLLA equimolar blend with high molecular weight ($M_w = 1 \times 10^6$ and 9.8×10^5, respectively) still could appear at the air−water interface. This value is much higher than the high critical molecular weight ($M_w = 1 \times 10^5$) reported by Tsuji et al.,[6] which is one of the basic conditions for PDLA/PLLA bulk stereocomplexation in the bulk from the melt or solutions. This phenomenon may be attributed to the cooperative effect of the increased segment mobility of PDLA and PLLA chains at the air−water interface and the increased probability of the parallel arrangements between PLLA and PDLA chain segments caused by the expanded state of molecular chains and compression. Second, the LB behavior of a PDLA/PLLA blend with lower molecular weight ($M_w = 4 \times 10^3$ and 3.2×10^3, respectively), which should favor the stereocomplexation process in the bulk

from the melt or solutions, shows LB behavior at the air−water interface distinct from that of the other higher molecular weight blends. The expanded phase behavior and IR data of D1/L1 at the low-pressure region indicate that polymer chains in such a low-molecular-weight D/L blend take a helical conformation rather than a random coil conformation at the air−water interface when the film is spontaneously cast on the surface of water.

AFM height images clearly disclosed the morphological changes of PDLA and PLLA equimolar blends of both high and low molecular weights at the air−water interface induced by increasing the surface pressure of the monolayer. At the high-pressure region, the morphology of an LB multilayer with high molecular weight is more smooth and ordered than that prepared with a low-molecular-weight D/L blend. Therefore, for a variety of applications, there is the potential to prepare an ordered ultrathin film with integrity of the PDLA/PLLA stereocomplex with high-molecular-weight polymer pairs. Of particular note, the unchanged height difference at 1.2−1.3 nm between the two phases, which is consistent with the diameter of the 3_1-helical chain of PDLA and PLLA, provides direct evidence for the bilayer mechanism of the phase transition in the plateau region.

Acknowledgment. The financial support of the Outstanding Youth Fund (Grant No. 20425414) and the National Natural Science Foundations of China (Grant Nos. 50521302, 20574079, and 20423003) is gratefully acknowledged. The encouragement and support of Professor Dr. Yoshito Ikada, Suzuka University of Medical Science, for this study are greatly appreciated. J.Z. thanks the Japan Society for the Promotion of Science (JSPS) for financial support.

References and Notes

(1) Vert, Ml.; Feijen, J.; Albertsson, A.; Scott, G.; Chiellini, E. *Biodegradable Polymers and Plastics*; The Royal Society of Chemistry: Cambridge, U.K., 1992.
(2) Doi, Y.; Fukuda, K. *Biodegradable Plastics and Polymers*; Elsevier: Amsterdam, 1994.
(3) Hollinger, J. O. *Biomedical Applications of Synthetic Biodegradable Polymers*; Studies in Polymer Science 12; CRC Press: Boca Raton, FL, 1995.
(4) Postema, A. R.; Pennings, A. J. *J. Appl. Polym. Sci.* **1989**, *37*, 2351.
(5) Ikada, Y.; Jamshidi, K.; Tsuji, H.; Hyon, S.-H. *Macromolecules* **1987**, *20*, 904.
(6) Tsuji, H.; Hyon, S.-H.; Ikada, Y. *Macromolecules* **1991**, *24*, 5651.
(7) Tsuji, H.; Hyon, S.-H.; Ikada, Y. *Macromolecules* **1991**, *24*, 5657.
(8) Tsuji, H.; Hyon, S.-H.; Ikada, Y. *Macromolecules* **1992**, *25*, 2940.
(9) Brochu, S.; Prud'homme R. E.; Barakat, I.; Jerome, R. *Macromolecules* **1995**, *28*, 5230.
(10) Tsuji, H.; Ikada, Y. *Macromolecules* **1992**, *25*, 5719.
(11) Tsuji, H.: Tezuka, Y. *Biomacromolecules* **2004**, *5*, 1181.
(12) Okihara, T.; Tsuji, M.; Kawaguchi, A.; Katayama, K.; Tsuji, H.; Hyon, S.-H.; Ikada, Y. *J. Macromol. Sci., Phys.* **1991**, *B30*, 119.
(13) Kobayashi, J.; Asahi, T.; Ichiki, M.; Okikawa, A.; Suzuki, H.; Watanabe, T.; Fukada, E.; Shikinami, Y. *J. Appl. Phys*. **1995**, *77*, 2957.
(14) Hoogsteen, W.; Postema, A. R.; Pennings, A. J.; ten Brinke, G.; Zugenmaier, P. *Macromolecules* **1990**, *23*, 634.
(15) Sasaki, S.; Asakura, T. *Macromolecules* **1996**, *29*, 7460.
(16) Brizzolara, D.; Cantow, H.-J.; Diederichs, K.; Keller, E.; Domb, A. J. *Macromolecules* **1996**, *29*, 191.
(17) Zhang, J. M.; Sato, H.; Tsuji, H.; Noda, I.; Ozaki, Y. *Macromolecules* **2005**, *38*, 1822.
(18) Brinkhuis, R. H. G.; Schouten, A. J. *Macromolecules* **1992**, *25*, 2725.
(19) Brinkhuis, R. H. G.; Schouten, A. J. *Macromolecules* **1992**, *25*, 2732.
(20) Brinkhuis, R. H. G.; Schouten, A. J. *Macromolecules* **1993**, *26*, 2514.
(21) Brinkhuis, R. H. G.; Schouten, A. J. *Macromolecules* **1992**, *25*, 6173.
(22) Bourque, H.; Laurin, I.; Pézolet, M.; Klass, J. M.; Lennox, R. B.; Brown, G. R. *Langmuir* **2001**, *17*, 5842.
(23) Klass, J. M.; Lennox, R. B.; Brown, G. R.; Bourque, H.; Laurin, I.; Pézolet, M. *Langmuir* **2003**, *19*, 333.
(24) Pelletier, I.; Pézolet, M. *Macromolecules* **2004**, *37*, 4967.
(25) Brinkhuis, R. H. G.; Schouten, A. J. *Macromolecules* **1991**, *24*, 1487.
(26) Biegajski, J. E.; Cadenhead, D. A.; Prasad, P. N. *Macromolecules* **1991**, *24*, 298.
(27) Brinkhuis, R. H. G.; Schouten, A. J. *Macromolecules* **1991**, *24*, 1496.
(28) Kister, G.; Cassanas, G.; Vert, M. *Polymer* **1998**, *39*, 267.
(29) Lambeek, G.; Vorenkamp, E. J. Schouten, A. J. *Macromolecules* **1995**, *28*, 2023.
(30) Urban, M. W.; Provder, T.; Eds. Multidimensional Spectroscopy of Polymers. *Vibrational, NMR, and Fluorescence Techniques*; ACS Symposium Series 598; American Chemical Society: Washington, DC, 1995.
(31) Sawai, D.; Takahashi, K.; Sasashige, A.; Kanamoto, T. *Macromolecules* **2003**, *36*, 3601.
(32) Gaines, G. L., Jr. *Insoluble Monolayers at Liquid Gas Interfaces*; Interscience: New York, 1966.
(33) Llopis, J.; Subirana, J. A. *J. Colloid Sci*. **1961**, *16*, 618.
(34) Kikkawa, Y.; Fujita, M.; Abe, H.; Doi, Y. *Biomacromolecules* **2004**, *5*, 1187.
(35) Tsuji, H.; Ikada, Y.; Hyon, S.-H.; Kimura, Y.; Kitao, T. *J. Appl. Polym. Sci.* **1994**, *51*, 337.
(36) Yoo, K. H.; Yu, H. *Macromolecules* **1989**, *22*, 4019.
(37) Tsuji, H. *Polymer* **2002**, *43*, 1789.

BM060043T